LWT - Food Science and Technology 161 (2022) 113345

Contents lists available at ScienceDirect

LWT

journal homepage: www.elsevier.com/locate/lwt

Broadband Dielectric Spectroscopy (BDS) investigation of molecular relaxations in durum wheat dough at low temperatures and their relationship with rheological properties

Fabio Fanari [a], Ciprian Iacob [b,c], Gianluca Carboni [d], Francesco Desogus [a,*], Massimiliano Grosso [a], Manfred Wilhelm [b]

[a] Department of Mechanical, Chemical and Materials Engineering, University of Cagliari, 09123, Cagliari, Italy
[b] Institute for Chemical Technology and Polymer Chemistry, Karlsruhe Institute of Technology (KIT), 76131, Karlsruhe, Germany
[c] National Research and Development Institute for Cryogenic and Isotopic Technologies, Valcea, 240050, Romania
[d] Agris Sardegna - Agricultural Research Agency of Sardinia, Cagliari, Italy

ARTICLE INFO

Keywords:
Broadband dielectric spectroscopy
Dough rheology
Compliance
Durum wheat
Dielectric relaxations

ABSTRACT

Broadband Dielectric Spectroscopy (BDS) was used to study the dielectric relaxation processes of semolina doughs. The dielectric properties were analyzed as a function of water content, and, additionally, the effects of NaCl presence and semolina characteristics were investigated. The dough was prepared using three different varieties of semolina. BDS measurements were conducted using a custom-made Rheo-dielectric tool composed of a Broadband Dielectric/Impedance Spectrometer connected to a strain-controlled rheometer. The temperature range investigated was from −135 °C to 25 °C, with a step of 5 °C, while the frequency range was 10^{-1} – 10^{7} Hz. Dielectric spectroscopy turned out to be a valuable technique for dough characterization. It is capable to distinguish the carbohydrates contribution and the different interactions between water and dough components. Moreover, this unique combination allows assessing correlations between rheological and dielectric properties, like the compliance of dough as a function of the relaxation processes and the influence of semolina components.

1. Introduction

Durum wheat is the most appropriate raw material for making pasta; it is one of the hardest varieties of wheat, the milling of which produces coarse particles called semolina (Sicignano, Di Monaco, Masi, & Cavella, 2015). Although common wheat is preferred to durum one in the bread-making, in the last years the production and consumption of bread made of durum wheat have been increased (Mefleh et al., 2019). This is due to the several advantages that this kind of bread presents compared to common bread (e.g. yellowish colour, appreciated characteristic taste and odour, fine uniform crumb structure, higher content of proteins, and a longer shelf-life) (Ficco et al., 2017; Pandino, Mattiolo, Lombardo, Lombardo, & Mauromicale, 2020).

The quality of semolina doughs is strongly influenced by the interactions among the ingredients in the presence of water and salt (Fanari, Carboni, Grosso, & Desogus, 2020; Torbica, Mocko Blažek, Belović, & JanićHajnal, 2019). Several studies concern the influence of ingredients and semolina variety on the rheological properties of doughs and, in the most recent literature, new insight into the dough microstructure is presented (Bonilla, Erturk, & Kokini, 2020; Bonilla, Erturk, Schaber, & Kokini, 2020). The role of gluten in conditioning the texture and rheological properties is well known, and due to the formation of a viscoelastic network during hydration and mixing (Bonilla, Schaber, Bhunia, & Kokini, 2019). However, also starch has a relevant influence on the rheological properties of dough. Indeed, even if it has no significant network-forming properties, it is embedded into the gluten network, it has a large volume fraction and interacts, to a certain extent, with the surrounding matrix (Brandner, Becker, & Jekle, 2019). For example, it was found that the viscosity increases with the damaged starch content due to the higher amount of absorbed water (Barak, Mudgil, & Khatkar, 2014). Even the particle size showed effects on viscoelastic properties of durum wheat doughs (Edwards, Dexter, & Scanlon, 2002). On the other side, semolina doughs have been less studied concerning their dielectric properties.

Broadband Dielectric Spectroscopy (BDS) is a non-invasive technique useful to characterize the distribution and influence of the main

* Corresponding author.
E-mail address: francesco.desogus2@unica.it (F. Desogus).

https://doi.org/10.1016/j.lwt.2022.113345
Received 9 October 2021; Received in revised form 3 February 2022; Accepted 9 March 2022
Available online 16 March 2022

polar components (electrical dipoles within the molecules) which are present in the system (Kang, Lu, Cheng, & Jin, 2015), e.g. water. This technique has great importance in food and in the biomaterials systems field since it is able to discriminate between the free and the various coexisting bond water states in the material and relates the different mobility to the structural and textural changes (Li, Zhang, & Yang, 2019; Nielsen et al., 2016). Various non-equilibrium states and the corresponding transitions, resulting from molecular movements (translation and rotation) and flow dynamics, could be observed during the processing and storage of bakery products (Wang & Zhou, 2017). The rates of these changes are dependent on molecular mobility, product formulation, water activity, storage condition, processing parameters, etc. (Slade & Levine, 1995). Despite the potentiality of this spectroscopic technique, the knowledge and understanding of the dielectric properties of food components are so far quite limited. An important parameter that can be determined using dielectric spectroscopy is the glass transition temperature (Tg), a concept originally developed and applied for synthetic polymers. Meanwhile, it has been applied to many food products to predict their stability (Balasubramanian, Devi, Singh, D Bosco, & Mohite, 2016). Regarding dough, in the literature, we can find few studies related to dough T_g determination. In several publications (Akbarian, Koocheki, Mohebbi, & Milani, 2016; Ding et al., 2015; Matuda, Pessôa Filho, & Tadini, 2011; Meziani et al., 2011), a relaxation process was detected at around −40 °C, through differential scanning calorimetry (DSC), and it was associated with the dough glass transition. However, one should remark that dough and foods are mixtures of different components that have a spatial heterogeneity at longer length scales (e.g. > 5 nm), consequently, it is not possible to define a single glass transition temperature, but rather a temperature range, the width of which is controlled by the dynamic and spatial heterogeneity of the system (Böhmer et al., 1998; Heuer, Wilhelm, Zimmermann, & Spiess, 1995; Tracht et al., 1998). This fact generates the necessity to investigate better the relaxation processes in the dough since its dielectric properties are strongly related to its microstructure, mostly consisting of the so-called gluten network (Miller & Hoseney, 2008). Also starch has a relevant role in determining the microstructural and rheological characteristics of durum wheat dough, but it is often underestimated compared to that of gluten. Indeed, especially when semolina is taken into account, the surface characteristics of starch granules may affect the protein–starch interaction and the viscoelastic behaviour of the dough (Edwards et al., 2002). Dielectric spectroscopy has shown the presence of several molecular relaxations in starch. Butler and Cameron (Butler & Cameron, 2000) reported a relaxation in the range from −120 to −90 °C (denoted with 'γ_1'), obeying the Arrhenius law, as reflected by single activation energy, and another relaxation at slightly lower temperatures (denoted with 'γ_2'), which was observed only in starch with low water contents. Roudaut et al. (Roudaut, Maglione, Van Dusschoten, & Le Meste, 1999) also observed a secondary relaxation, with apparent activation energy (E_a) of about 50 kJ/mol, between −60 and −40 °C (depending on the frequency), which was related to the carbohydrate ingredients (sucrose and starch) of bread. Also non-starch polysaccharides, notwithstanding they represent only about 2–2.5% of the flour mass (Migliori & Gabriele, 2010), have a great influence on dough properties (Bibi, Villain, Guillaume, Sorli, & Gontard, 2016). Ross (Roos, 1993) reported various glass transition temperatures of mono- and di-saccharides, and alditols, in the range between −40 and −70 °C, at which several works previously reported associated relaxation processes. Laaksonen and Roos (Laaksonen & Roos, 2001a), using dielectric analysis at 0.1 Hz, found a T_g of −33 °C and two relaxation processes, one β relaxation at −85 °C and one γ process at −148 °C. In another publication (Laaksonen & Roos, 2000), the same authors noticed that these temperatures increase as frequency increases and they reported four relaxation processes: one first-order phase transition associated with ice melting ($E_a = 266.4$ kJ/mol), another one with a glass transition ($E_a = 97.1$ kJ/mol), one single β relaxation ($E_a = 63.0$ kJ/mol) and one single γ process ($E_a = 31.5$ kJ/mol). The results were obtained through dielectric spectroscopy, which revealed much more sensitive in observing thermal transitions with respect to Differential Scanning Calorimetry (DSC) and Dynamic Mechanical Analysis (DMA). However, even through DMA, at frequencies of 1, 5 and 10 Hz, Ribotta and Le Bail (Ribotta & Le Bail, 2007) found a relaxation process at around −7 °C, corresponding to melting of ice, an α-relaxation (glass transition) at around −35 °C and a β-relaxation at around −78 °C, while Laaksonen and Roos (Laaksonen & Roos, 2001b) reported a β relaxation at about −80 °C and a γ process in the temperature range from −100 °C to −136 °C at 2.5, 5 and 10 Hz.

Despite starch being contained in high amounts in baked doughs, the main component that influences the dielectric properties is water due to its high mobility, large dipole moment, and ability to act as a plasticizer. Goedeken et al. (Goedeken, Tong, & Virtanen, 1997) reported that the dielectric properties are related not only to the water content but also to the interaction forces between the other components of the material and the dissolved water molecules. According to this, any influence of the starch kind, or crystallinity, is overshadowed by the one of bound water dipoles rotational motion (Roudaut, Simatos, Champion, Contreras-Lopez, & Le Meste, 2004). Water plasticizing properties are well known and, due to this characteristic, moisture content of about 30% wt. Is sufficient to reduce the T_g of many carbohydrates and proteins, including starch and gluten, up to about −10 °C (Levine & Slade, 1990). Moreover, water influences the temperature effect on the dough dielectric properties. These results highlight the need for testing samples with a known and controlled water content. Water dielectric relaxations can be observed at high frequencies higher than 100 MHz (Popov, Ishai, Khamzin, & Feldman, 2016) if the local motion of the water is not substantially constrained. However, the vibration of water atoms or bonds and the local reorientation of small groups of atoms are still possible at lower frequencies, even in the glassy state (Chan, Pathmanathan, & Johari, 1986), and these movements facilitate the structural relaxations (Perera, 2002).

Furthermore, the addition of salt, specifically NaCl, affects the dielectric properties of dough. In more detail, the salt presence significantly increases the dielectric loss (ε") because it generates an additional conductivity due to the ion migration (Fanari, Muntoni, Dachena, Carta, & Desogus, 2020). Indeed, the number of dissolved ions is the most important factor affecting the absolute values of the dielectric loss (Kim & Cornillon, 2001). The ion concentration directly influences water mobility since only the water molecules having sufficient mobility can participate in dissolving salts. In addition, other publications (Laaksonen, Kuuva, Jouppila, & Roos, 2002; Laaksonen & Roos, 2001a, 2003) showed that the presence of NaCl significantly decreases the dough T_g but also the temperature of the other relaxation processes, if the same mobility is considered.

The objective of the present study is to investigate the effect of ingredients (water and NaCl) and of the semolina composition on the dielectric relaxations occurring at low (sub-zero) temperatures in the dough. In particular, at these temperatures, according to the previous considerations, the dielectric response could be informative on carbohydrates and thus on their role in the definition of the rheological properties of dough, as gluten is expected to be not detectable in such conditions, and the water mobility is reduced as much as possible. Therefore, measuring and understanding the phase transitions and relaxation processes occurring in doughs at sub-zero temperatures, and finding possible correlations with rheological parameters, could be useful for understanding the role of carbohydrates on the mechanical properties of semolina doughs. This new knowledge could find application in the pasta and baking manufacturing, where optimisation of the product texture is crucial. So a more and more precise definition of the rheological characteristics of doughs is necessary. Even the manufacturing of frozen doughs could benefit from this information, which is useful for temperature optimisation to limit changes in the material. Moreover, information about the carbohydrate effects on the rheological properties of foods has the potential to be useful also in other

food sectors, e.g. in gluten-free productions, where the texture reveals to be even more critical.

2. Materials and methods

2.1. Sample preparation

For each sample, 300 g of semolina (three different varieties were used), distilled water, and sea salt, in different amounts, were kneaded using a measuring mixer type 350 (Brabender® GmbH, Duisburg, Germany). The mixing time was determined as the one required to reach the dough maximum strength point, as observed in previous investigations (Fanari et al., 2019; Fanari, Desogus, Scano, Carboni, & Grosso, 2020), and it was found to be 3–5 min, depending on the sample. The rotational mixing speed was set to 20 rpm to reduce the effect of structural breaks in the dough network. Three different types of semolina were investigated. Two are of non-commercial monovarietal species cultivated in the "S. Michele" experimental farm of the Agricultural Research Agency of Sardinia (AGRIS) in Ussana (Italy), resulting from the milling of Karalis and Cappelli grains. The third kind is a commercial blend acquired in the German retail stores (Gold Puder-Hartweizen Grieβ, Aurora Mühlen GmbH, Hamburg, Germany). It should be remarked that their properties are quite different in terms of protein and gluten content and gluten index, as can be seen in Table 1. Gluten index (GI) is a parameter providing information on both gluten quality and gluten quantity, and it expresses the weight percentage of the wet gluten remaining on a sieve after automatic washing with a salt solution and centrifugation (Oikonomou, Bakalis, Rahman, & Krokida, 2015). The semolina protein content was determined by the nitrogen combustion method (ISO 16634-2:2016, 2016) using a Leco FP528 nitrogen analyzer (LECO, Stockport, UK). The gluten content and the gluten index (GI) of semolina were determined following the ICC standard method No. 158 (ICC, 1995) by using the Glutomatic 2200 system (Perten Instruments AB, Huddinge, Sweden). Table 2 reports the mass percentual composition of the samples, with respect to the semolina weight, in terms of water and salt content.

2.2. Dielectric characterization

For the dielectric measurements, the sample was placed between two custom-made invar-steel parallel plate electrodes of 25 mm diameter, mounted on an ARES-G2 strain-controlled rheometer (TA Instruments, New Castle, USA). The initial gap in the measurement was 1 mm between the plates. The distance was adjusted during the experiment to maintain the normal force at around 1 N. This is important because, during the freezing and defrosting processes, the sample changes its volume. Thus, the spacing during the experiments resulted from 0.8 to 1.2 mm. The experimental setup is shown in Fig. 1. As soon as the sample loading was completed, the dough was quickly cooled to −135 °C using the rheometer temperature control system. This operation was conducted in the fastest way to avoid the sample's drying, limit the growth of frozen water crystals, and keep the structure and properties of starch unmodified (Yang et al., 2021). After the thermal stabilization, the dielectric analysis was carried out step by step by raising the sample temperature by 5 °C for each step, from −135 to +25 °C. For each temperature step, after thermal stabilization was reached, a dielectric measurement was performed.

Table 1
Semolina varieties characteristics (means ± STD); values with different letters in the same column are significantly different (p-value ≤ 0.05).

	Proteins (%)	Gluten (%)	Gluten Index (%)
Cappelli (CAP)	14.0 ± 0.17 [a]	12.3 ± 0.30 [a]	16.5 ± 2.35 [a]
Karalis (KAR)	11.0 ± 0.05 [b]	7.0 ± 0.34 [b]	98.4 ± 0.79 [b]
Commercial (COM)	12.0 ± 0.12 [c]	8.3 ± 0.27 [c]	90.3 ± 2.12 [c]

Table 2
Composition of the dough reported as wt.% based on semolina weight.

Sample	Semolina variety	Water (wt.%)	Salt (wt.%)
CAP40	Cappelli	40	0
CAP50	Cappelli	50	0
CAP60	Cappelli	60	0
KAR40	Karalis	40	0
KAR50	Karalis	50	0
KAR60	Karalis	60	0
COM40	Commercial	40	0
COM50	Commercial	50	0
COM60	Commercial	60	0
CAP50S	Cappelli	50	1.5
KAR50S	Karalis	50	1.5
COM50S	Commercial	50	1.5

Dielectric measurements were carried out by a Novocontrol Technologies Alpha High-Resolution Broadband Dielectric/Impedance Spectrometer (Montabaur, Germany), within the frequency (f) range 10^{-1} - 10^{7} Hz, connected with the strain-controlled rheometer parallel plates in a custom-made experimental apparatus already described in previous works (Hyun, Höfl, Kahle, & Wilhelm, 2009; Meins, Dingenouts, Kübel, & Wilhelm, 2012). The signal voltage to generate the electric field was set to 0.5 V. Then, phase and state transitions of wheat dough samples were studied by monitoring the imaginary part of the complex permittivity (ε''), the dielectric parameter tan(δ) ($\tan(\delta) = \varepsilon''/\varepsilon'$) and the real part of the conductivity σ' as a function of the temperature (ε' is the real part of the permittivity). The frequency dependent ε'' is particularly important since its value is proportional to the conductance and can be related to the energy required to align dipoles or allow the ions movement so that it can be linked to the relaxation processes. To clearly see these relaxation processes, notwithstanding the Ohmic conduction influence, due to the presence of ions, in the cases of samples without salt, it is possible to apply the Kramers–Kronig rule reported in Equation (1) (Wübbenhorst & Van Turnhout, 2002). This relationship, which is a function of the angular frequency ω, defines an imaginary value ε''_{der}, which approximately equals the one of the Ohmic-conduction-free dielectric loss (ε''_{rel}) for rather broad peaks, like those of the α-transition or the secondary relaxations (Steeman & van Turnhout, 1994).

$$\varepsilon''_{der} = -\frac{\pi}{2}\frac{\partial\varepsilon'(\omega)}{\partial[\ln\omega]} \tag{1}$$

A comparison between measured values of ε'' and the calculated values of ε''_{der} for a COM50 sample is shown in Fig. 2a. The derivative method (Equation (1)) emphasizes the ε'' peaks, in correspondence to the relaxation frequencies, making their individuation and analysis easier.

The relaxation frequency was then calculated as the peak frequency of ε''_{der}. To do this, the dependence of ε''_{der} on frequency was firstly modeled by using the Havriliak-Negami (HN) relationship (Havriliak & Negami, 1967; Volkov, Koposov, Perfil'ev, & Tyagunin, 2018):

$$\varepsilon'' = \Delta\varepsilon\left[1 + 2\cdot(\omega\cdot\tau_{HN})^{\alpha}\cdot\cos\left(\frac{\pi\alpha}{2}\right) + (\omega\cdot\tau_{HN})^{2\alpha}\right]^{\left(-\beta/2\right)}\sin(\beta\varphi)\Bigg] \tag{2}$$

The parameters α and β are the fractional HN shape parameters (corresponding to high-frequency skewness and breadth, respectively); Δε is the relaxation strength, that is the difference between the static (low frequency) permittivity and the permittivity at the high-frequency limit (ε_s-ε_∞); φ is a parameter obtainable by Equation (3); τ_{HN} is the relaxation time associated with the characteristic frequency ω_{HN}, which is related to the frequency of maximum loss (ω_{max}) by Equation (4).

$$\varphi = arctan\frac{\sin(\alpha\pi/2)}{(\omega\tau_{HN})^{-\alpha} + \cos(\alpha\pi/2)} \tag{3}$$

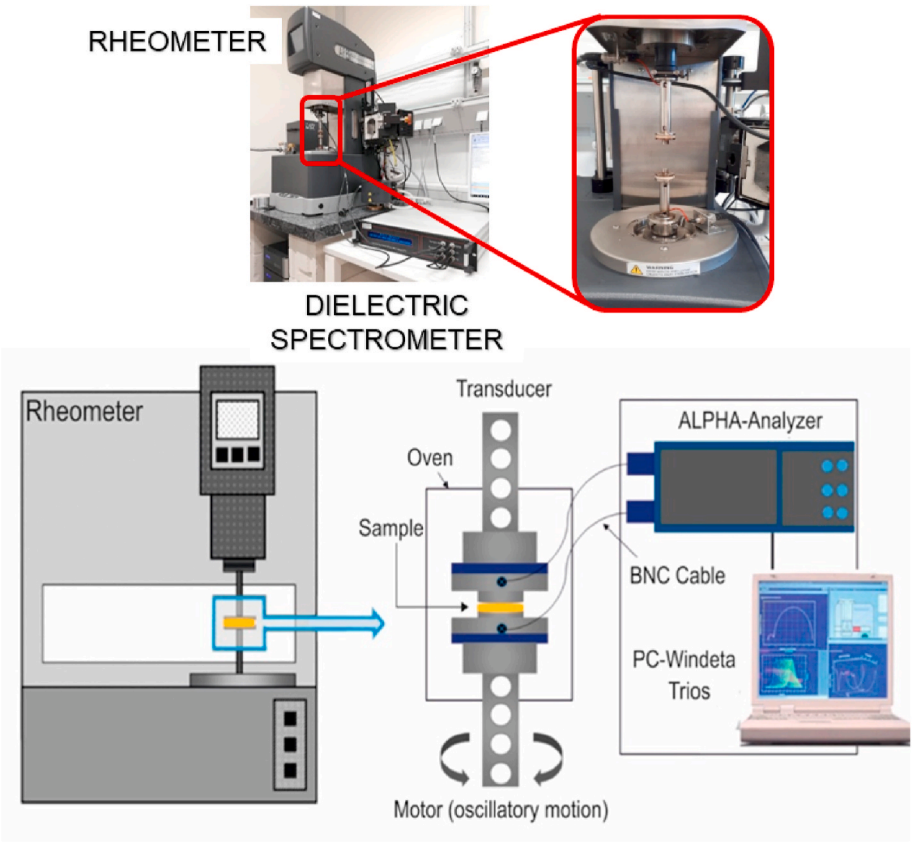

Fig. 1. *Set-up (a) and (b) a scheme of the unique rheology-dielectric spectroscopy combination* (Hyun et al., 2009).

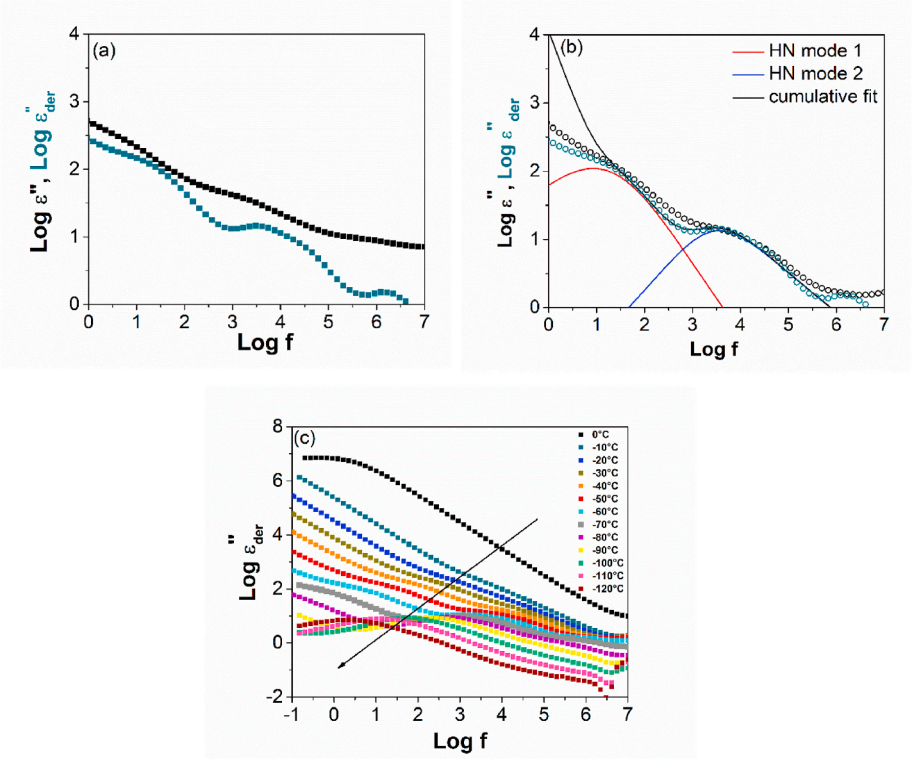

Fig. 2. a) Comparison between ε'' (black) and ε''_{der} (green) values at −50 °C for COM50 sample; it shows that the derivative method (Equation (1)) enhances the peaks in ε''. b) Example of fitting with Havriliak-Negami relationship for COM50. c) ε''_{der} as a function of frequency (in Hz) at different temperatures as indicated. (For interpretation of the references to colour in this figure legend, the reader is referred to the Web version of this article.)

The parameters calculated by fitting Equation (2) (an example of the fitting is shown in Fig. 2b) were used in Equation (4) to calculate the frequency corresponding to the maximum of the ε'' function (Schönhals & Kremer, 2003):

$$\omega_{max} = \omega_{HN}\left[\frac{\left(sin\frac{\alpha\beta\pi}{2+2\beta}\right)}{\left(sin\frac{\alpha\pi}{2+2\beta}\right)}\right]^{-1/\alpha} \quad (4)$$

Relaxations can be represented on mobility maps which are displayed as the logarithm of the relaxation frequency as a function of the reciprocal values of the absolute temperature (Arrhenius activation). This can be used to characterize the different motions taking place in a material at a given temperature and frequency range. Then, the apparent activation energy of relaxations was evaluated by Equation (5), describing an Arrhenius type activation behaviour (Iacob, Yoo, & Runt, 2018):

$$\omega_\beta(T) = \omega_0 \cdot e^{-\frac{E_a}{RT}} \quad (5)$$

where ω_β is the relaxation angular frequency, E_a is the apparent activation energy; R is the gas constant, T is the absolute temperature, and ω_0 is a constant, having the meaning of a maximum possible angular relaxation frequency at infinite temperatures. The sensitivity analysis concerning frequency allows the discrimination between relaxation processes and structural changes such as melting or crystallization. So, the values of the activation energies of the samples were calculated for each of them to enhance the difference between the relaxation processes occurring and relate them to the difference in the samples. From Fig. 2c it is possible to observe how the frequency peaks in ε''_{der} are moving to lower frequencies as temperature decreases.

2.3. Rheological characterization

The rheological experiments were performed using the same device, already described in the previous subsection 2.2, equipped with standard 25 mm plates and a Peltier-based system for temperature control. Immediately after the kneading process, a piece of dough was loaded on the rheometer, compressed to a gap of 2 mm, and then left to rest for 15 min to allow the material relaxation, as suggested in the literature (Phan-Thien & Safari-Ardi, 1998). To prevent evaporation and, consequently, drying of the sample, a layer of silicon oil was applied to its edge. The temperature in the rheometer was kept constant at 25 °C. Then, creep tests were performed applying a 50 Pa constant stress to the sample to stay in the linear viscoelastic region, according to the values of yield stress limit (70–100 Pa) determined through amplitude sweeps previously performed. This value also agrees with the values used to perform creep experiments on dough in other studies found in the literature (Döring, Nuber, Stukenborg, Jekle, & Becker, 2015; Mironeasa & Codină, 2019; Moreira, Chenlo, Torres, & Rama, 2014). The stress was applied for 150 s. Each test for each sample was repeated three times, and the mean value was considered in the present study. The compliance J, which is the ratio between deformation and applied stress, was measured against time to evaluate the rheological properties of the samples. The dependence of J on time is, in general, described in terms of mechanical models composed of basic elements. One of the most used is the Burgers model, which works as a Kelvin and a Maxwell model placed in series. Mathematically, it can be written as (Mainardi & Spada, 2011):

$$J(t) = J_0 + J_m\left(1 - e^{-\frac{t}{\tau}}\right) + \frac{t}{\eta_0} \quad (6)$$

The model parameters are the steady-state viscosity η_0, the instantaneous and delayed compliance, respectively J_0 and J_m, and the delay time τ that indicates how long the material takes to settle to deformation. Many applications of this model to bread dough characterization can be found in the literature (Beck, Jekle, & Becker, 2012; Mironeasa & Codină, 2019; Sun, Koksel, Nickerson, & Scanlon, 2020).

3. Results

3.1. Dielectric characterization

The ε'' spectra were analyzed, and the relaxation peaks were detected in terms of peak frequency. All the spectra at temperatures higher than 0 °C present a deflection in the ε'' values, erroneously attributable to the α-segmental relaxation process. This peak is, instead, related to the conductivity relaxation and at around 0 °C is significantly affected by water crystallization. The effect of this process can be observed from Fig. 3, where tan(δ) and σ' for samples with 50% of water and no salt (CAP50, COM50, and KAR50) at different temperatures are reported as an example. The static conductivity σ_0, detectable from the plateau in σ', sensibly decreases when the temperature goes to 0 °C and sub-zero values. Consequently, also the corresponding peak in tan(δ) is decisively moving at lower frequencies. In this range of temperatures also the α-segmental relaxation process is screened by the dc conductivity and water crystallization peak.

For each tested temperature, together with tan(δ) and σ_0, the relaxation frequencies are reported as a function of inverse temperature in Fig. 4a for CAP50, KAR50, and COM50 samples. It is possible to see that only two relaxation processes are revealed. Both relaxations occur at temperatures lower than the temperatures characteristic of the crystallization process. One process at very low temperatures, classifiable as γ relaxation, and another one at higher temperatures, attributable to a β relaxation, can be found. Their trend suggests a single motion with Arrhenius type behaviour of the relaxation frequency with respect to the temperature. Thus, for each sample, the relaxation frequency data as a function of temperature were fitted using Equation (5) (Arrhenius dependence law). Fig. 4 shows, as an example, the regressions for CAP50, KAR50, and COM50, while the mobility map and respective regressions for the other samples are shown in Figure A1 reported in Appendix A. Additionally, in Table 3, the calculated values of activation energy for β (β E_a) and γ (γ E_a) relaxations, for all the samples, and the 95% confidence intervals, are reported. Table 4 reports the values of the statistical parameters of the regressions. The computed statistics (R^2 and MSE) suggest that the exponential Arrhenius dependence reveals to be a simple, though effective, method to describe the relaxation frequency as a function of temperature, with a value of Adj-R^2 higher than 0.99 in most cases. Moreover, the only presence of an Arrhenius dependence advises that there are no contributions of a multimode glass transition, so it is not possible to calculate any T_g since the glass transitions usually show a different behaviour, following a Vogel−Fulcher−Tammann type temperature dependence (Iacob et al., 2018).

The trend of tan(δ) as a function of the temperature for a fixed frequency (100 Hz) is shown in Fig. 5 for three samples chosen as an example, and for the other samples in Figures A2-A3 (Appendix A). The experimentally determined tan(δ) values in the temperature range investigated show three main peaks for all the samples. The correspondent temperature and tan(δ) height values of these peaks are reported in Table 5 for water crystallization, (W_CP), β (βP), and γ (γP) processes, respectively. The dielectric excitation frequency of 100 Hz was chosen as it allows to clearly see all the three characteristic peaks identified (Laaksonen et al., 2002). Indeed, at lower frequencies, peaks are not clearly detectable, especially the ones at a higher temperature. The first peak in tan(δ) is located at about 0 °C, and it is likely related to water crystallization and not to an α relaxation process. This theory is supported by visual inspection of Fig. 4 and A1, where conductivity and tan(δ) relaxation peaks are reported as a function of inverse temperature. In fact, a steep fall in correspondence of the water freezing point (0 °C) is indeed observed. Another peak is visible in the range between −60 and −40 °C, which probably corresponds to the β process observed

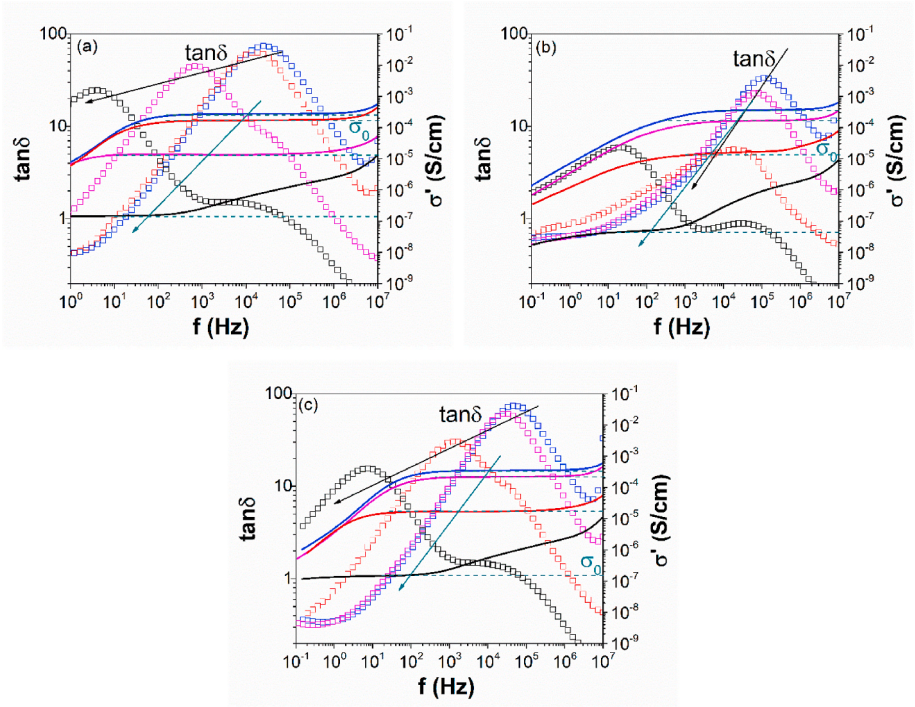

Fig. 3. Tan(δ) and σ' as a function of frequency (logarithmic scale) for (a) CAP50, (b) KAR50 and (c) COM50. The values are reported at different temperatures: 25 °C (blue), 10 °C (magenta), 0 °C (red), −10 °C (black). The black line follows the tan(δ) peak moving while the green line is representative of the σ0 drop. (For interpretation of the references to colour in this figure legend, the reader is referred to the Web version of this article.)

in the mobility maps. The other peak which was identified is precisely located at −105 °C for all the samples and could be due to the γ relaxation previously detected in the mobility maps.

The influence of salt is appreciable when comparing the samples data without salt (COM50, KAR50, and CAP50) and with salt (COM50S, KAR50S, and CAP50S). Focusing on the data reported in Fig. 6 and Figure A1, an additional relaxation process is observed when salt is added for both COM and KAR samples. This additional relaxation (named γ_2) follows an Arrhenius type dependence on the temperature and has activation energy (γ_2 E_a) in the range of 80–90 kJ/mol. In the CAP50S sample, no additional relaxations were detected, probably because they are hidden by more dominant ones. In effect, the CAP samples are the only ones that are not significantly affected in any of the tan(δ) peaks. About the tan(δ) peak temperatures, a decrease of 20 °C in the β relaxation peak temperature can be observed for all the samples, while the other peaks show a shift in the order of ±5–10 °C. Moreover, for the KAR50S sample, as shown in Fig. 6, tan(δ) shows a very sharp additional peak (denoted with "i" in Fig. 6), at about −40 °C, due to the additional relaxation process observed in the mobility map, that probably is hidden by the higher β relaxation peak for CAP50S and COM50S, as it is observable in figure A3 (Appendix A).

3.2. Rheological characterization

Results are presented in Fig. 7, where compliance as a function of time for each semolina variety is shown. Results pertaining to CAP, KAR, and COM samples with different water amounts and salt addition are reported in Fig. 7a, 7b, and 7c, respectively. The main outcomes of this analysis are a weak influence of the water amount on the rheological properties for the CAP samples and, on the contrary, a high sensibility to water for the COM samples. On the other hand, KAR samples show intermediate rheological properties. Moreover, the salt addition has a mildly negative effect on the dough deformability, increasing the compliance values of KAR and COM samples while, in the case of CAP samples, it produces a considerable decrement of compliance, and, as a consequence, an increase in the strength of the dough network. Fig. 7d, instead, reports the semolina variety influence on the rheological properties. It is noticeable that the CAP50 sample presents the lowest compliance. CAP results to be the strongest semolina variety, followed by KAR, and COM turned out to be the weakest, with higher deformability.

Non-linear regression was accomplished on the compliance vs time data in order to calculate the Burgers model (Eq. (6)) parameters. Their values for each sample are reported in Table 6.

3.3. Statistical analysis

Pearson correlation coefficients were computed to evaluate correlations between rheological parameters and dielectric ones. Also correlation coefficients between these parameters and water content, protein amount, gluten amount, and gluten index were evaluated. Finally, statistical significance for all these correlations was evaluated through the p-value estimation. The results are reported in Table 7.

4. Discussion

4.1. Water crystallization

The water crystallization process was detected between 0 and -10 °C. This process provides information about the water state in the system.

The height of the tan(δ) peak shows a very weak and negative correlation with the total water content ($r = -0.18$). On the other hand, it shows a good and significant correlation with the semolina protein and gluten amount ($r > 0.76$). This means that the dielectric response is mostly due to the interactions between water molecules and the structural components of the dough, in other words to the bound water.

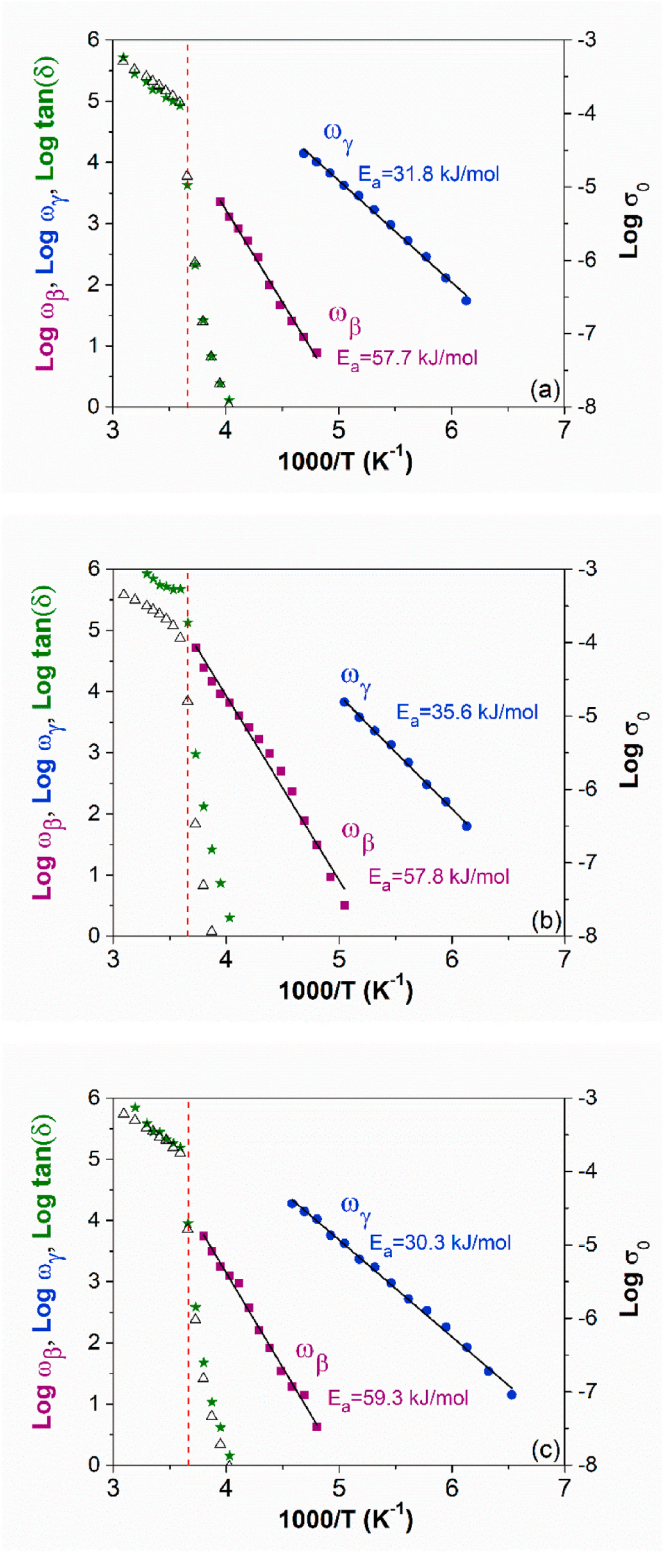

Fig. 4. Mobility map (ω in rad/s) and Arrhenius model regression with E_a values for (a) CAP50, (b) KAR50 and (c) COM50; the samples show two relaxation processes, γ with γ E_a around 30–35 kJ/mol and β with β E_a around 60–70 kJ/mol. Triangles represent tan(δ) while green stars σ_0 values. The red dashed line highlights the crystallization temperature, in correspondence of which a drop in tan(δ) is observable. (For interpretation of the references to colour in this figure legend, the reader is referred to the Web version of this article.)

Table 3
Activation energy (E_a) and 95% confidence interval for dough samples with different water amounts.

Sample	β E_a (kJ/mol)	γ E_a (kJ/mol)	γ_2 E_a (kJ/mol)
COM40	72.5 ± 2.8	33.7 ± 2.2	–
COM50	59.3 ± 3.5	30.3 ± 1.1	–
COM60	73.6 ± 2.2	31.5 ± 0.9	–
KAR40	74.5 ± 5.7	40.4 ± 1.0	–
KAR50	57.8 ± 4.2	35.6 ± 1.6	–
KAR60	62.8 ± 3.4	31.8 ± 1.5	–
CAP40	60.0 ± 6.9	36.0 ± 1.6	–
CAP50	57.7 ± 4.0	31.8 ± 1.4	–
CAP60	52.4 ± 4.1	31.8 ± 1.3	–
COM50S	57.1 ± 5.8	38.6 ± 1.0	87.9 ± 3.5
KAR50S	63.6 ± 6.1	39.5 ± 1.4	83.3 ± 1.8
CAP50S	66.9 ± 5.2	41.1 ± 1.2	–

Table 4
Statistical parameters of the regressions.

Sample	β E_a		γ E_a		γ_2 E_a	
	RMSE	Adj-R^2	RMSE	Adj-R^2	RMSE	Adj-R^2
COM40	0.056	0.995	0.051	0.994	–	–
COM50	0.089	0.992	0.058	0.996	–	–
COM60	0.047	0.998	0.059	0.997	–	–
KAR40	0.068	0.994	0.044	0.998	–	–
KAR50	0.160	0.984	0.035	0.997	–	–
KAR60	0.143	0.990	0.039	0.997	–	–
CAP40	0.283	0.942	0.061	0.996	–	–
CAP50	0.078	0.992	0.050	0.996	–	–
CAP60	0.054	0.992	0.055	0.996	–	–
COM50S	0.079	0.988	0.044	0.999	0.025	0.999
KAR50S	0.047	0.994	0.039	0.998	0.024	0.999
CAP50S	0.090	0.991	0.035	0.999	–	–

4.2. *β relaxation*

The β relaxation occurred in the temperature range between −40 °C and −70 °C and shows activation energy of about 50–75 kJ/mol. Occurrence of β relaxation phenomena was already observed, at similar temperatures and with similar activation energy values, also through DSC in low molecular weight carbohydrates (Roos, 1993) and through DMA in frozen wheat doughs (Laaksonen & Roos, 2000; 2001b).

The most likely explanation of this process is that it corresponds to the glass transition and is linked to a modification in the mobility of large portions of the amylose and amylopectin molecules. Indeed, these latter systems show similar behaviour, in terms of temperature range and values of activation energy for the relaxation, as reported in the literature at the same frequency of 100 Hz (Butler & Cameron, 2000). Other studies (Roudaut, Maglione, Van Dusschoten, & Le Meste, 1999; Scandola, Ceccorulli, & Pizzoli, 1991) related this relaxation also to dextran or pullulan. This leads to the more general explanation of the rotational motion of the hydroxyl groups present on the C_2, C_3, or C_6 of the glucosidic units. It is also further confirmed by specific studies concerning the dielectric relaxations of glucose (Chan et al., 1986).

Possible connections between gluten sub-units and β relaxation can almost certainly be excluded, mainly based on previous studies, which revealed that gluten does not show any relaxation in the same temperature range with respect to the present work, but only at higher temperatures, with a peak at 27 °C (Roudaut, Maglione, & Le Meste, 1999).

The height of tan(δ) peak is significantly and highly correlated with the semolina protein and gluten amount ($r > 0.71$), and also with W_CP ($r = 0.75$), while the correlation with the water content presents a low and negative coefficient ($r = -0.30$). The positive and significant correlation with W_CP suggests that the two processes are largely explainable in the same way, i.e. with the bound water (also the other correlations are similar to those of the water crystallization). Since gluten is not detected, one can assume that this bound water involves carbohydrate molecules.

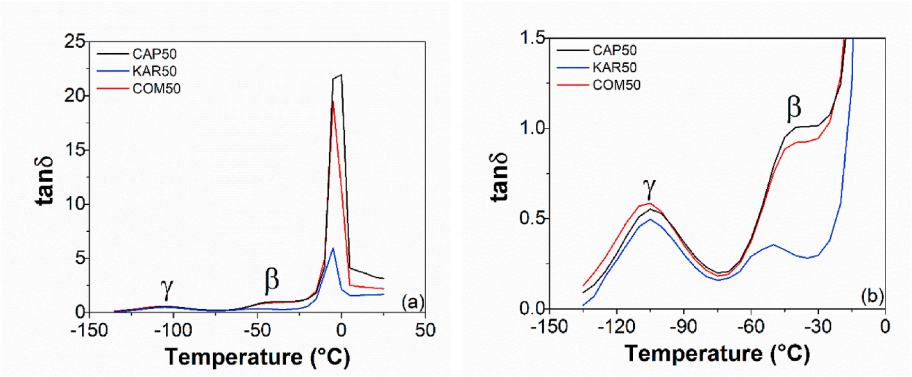

Fig. 5. Dielectric parameter tan(δ) as a function of temperature for CAP50, KAR50, and COM50 samples at 100 Hz (a) and enlargement of the β and γ relaxations zone (b).

Table 5
Dielectric tan(δ) peak values of water crystallization (W_CP), β relaxation (βP) and γ relaxation (γP), and corresponding temperature for all the samples, measured at 100 Hz.

	W_CP		βP		γP	
Sample	Tan(δ)	Temp. [°C]	Tan (δ)	Temp. [°C]	Tan (δ)	Temp. [°C]
COM40	19.076	−10	1.170	−60	0.465	−100
COM50	19.532	−5	0.886	−45	0.586	−105
COM60	2.464	0	0.308	−55	0.302	−115
KAR40	4.918	−5	0.412	−50	0.410	−105
KAR50	5.953	−5	0.356	−50	0.496	−105
KAR60	8.061	−5	0.473	−40	0.588	−105
CAP40	21.257	0	1.142	−40	0.472	−105
CAP50	21.951	0	1.006	−40	0.552	−105
CAP60	22.099	−5	0.949	−40	0.609	−105
COM50S	1.298	−10	0.104	−65	0.287	−105
KAR50S	9.368	−5	0.302	−70	0.449	−100
CAP50S	22.383	−10	1.018	−60	0.541	−100

As activation energy only depends on the energy status of the target groups, the low and negative correlation (r = – 0.31) observed with the water amount suggests that water can partially change the energy status of the target group (hydroxyl), and this could be explained with the possibility of interaction with water molecules (through hydrogen bonds). There is no clear explanation of the weak and negative correlation with the protein and gluten amount (r < – 0.36) unless it is considered that, in wheat flour, the amount of damaged starch is usually negatively well correlated with the gluten amount (Barak, Mudgil, & Khatkar, 2013). Considering that the damaged starch is the main responsible of the water absorption, a hypothesis could be the greater difficulty in the rotation of the hydroxyl groups due to the lower water relative availability with respect to the starch.

In the case of samples with added salt, the 20 °C temperature shifting in the β relaxation dielectric tan(δ) peak at 100 Hz, that was observed for all the samples, could be linked to the NaCl ability to reduce the transition temperatures of the unfrozen solute, as stated in a previous work (Laaksonen & Roos, 2001a).

4.3. γ relaxation

The γ relaxation occurred in the temperature range between −115 °C and −100 °C and shows activation energy of about 30–40 kJ/mol. The peak temperature corresponds to that shown in the literature (−112 °C) for wheat doughs at the same frequency of 100 Hz, and the same correspondence was found for the activation energy (31.5 kJ/mol) (Laaksonen & Roos, 2000). From this, the possibility that also gluten influences the γ relaxation process cannot be completely excluded, nor previous studies clearly assessing this aspect were found. However, other researchers (Butler & Cameron, 2000), testing only starch and not doughs, gave an explanation of this relaxation process, claiming that it is likely due to localized chain motions in starch molecules, probably enabled by the motion of the water molecules which are hydrogen-bonded to the amylose and amylopectin molecules, and that small-amplitude oscillations of the glucose rings about the (1–4)-α and (1–6)-α linkages are the most likely candidates. The similarity between the dielectric response in this work and ours makes the possibility of a gluten influence on the γ relaxation process very unlikely.

The height of the tan(δ) peak presents the weakest correlation with the semolina protein and gluten amount (r > 0.32), and also with the water amount (r = 0.18). Correlation with W_CP is high (r = 0.71), significant, and similar to the one between βP and W_CP. However, the correlation between γP and βP is much lower (r = 0.38) and not significant. This could be supported by the fact that the two processes are

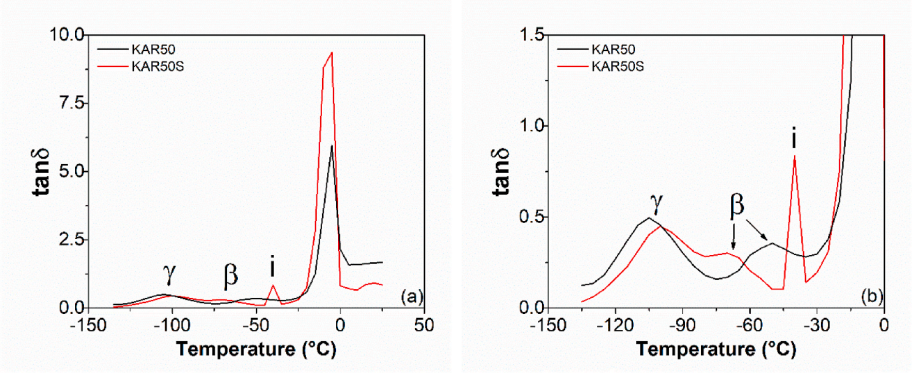

Fig. 6. Tan(δ) as a function of temperature for samples KAR50 and KAR50S at 100 Hz (a) and enlargement of the β, γ, and i relaxations zone (b).

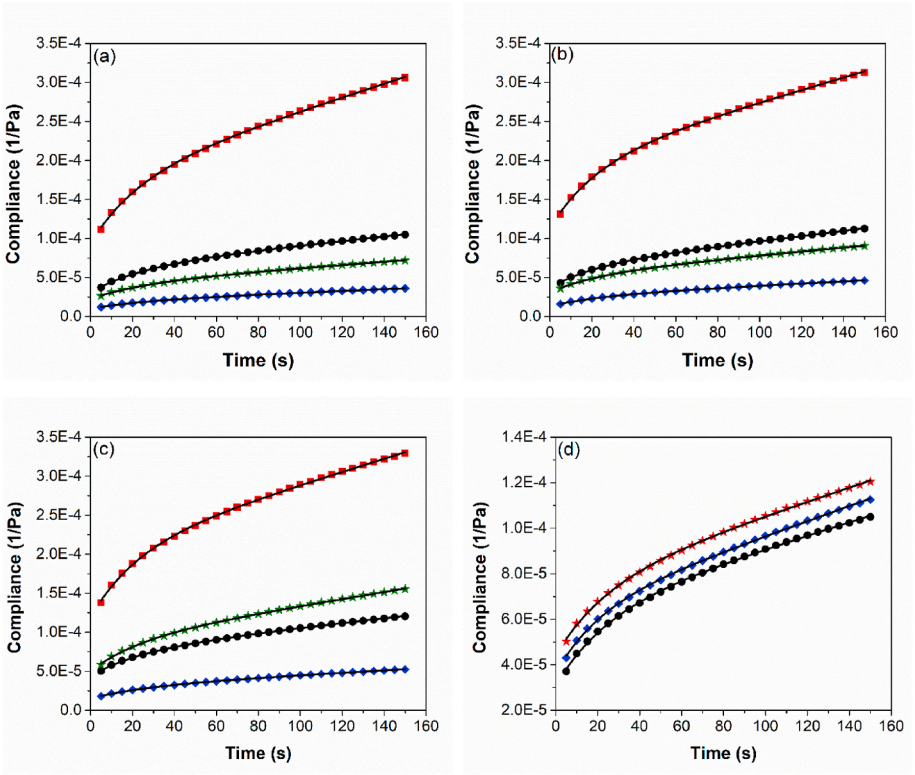

Fig. 7. Compliance against time comparisons among (a) CAP40 (blue), CAP50 (black), CAP60 (red) and CAP50S (green); (b) KAR40 (blue), KAR50 (black), KAR60 (red) and KAR50S (green); c) COM40 (blue), COM50 (black), COM60 (red) and COM50S (green); (d) CAP50 (black), KAR50 (blue) and COM50 (red). Data were acquired by creep tests applying a 50 Pa stress at 25 °C and modeled with Burgers model (black lines represent the model regression). (For interpretation of the references to colour in this figure legend, the reader is referred to the Web version of this article.)

Table 6
Parameters of the Burgers model estimated for the different samples.

Sample	J_0 (Pa^{-1})	J_m (Pa^{-1})	τ (s)	η_0 (Pa • s)	Adj-R2
KAR40	$1.35{\cdot}10^{-5}$	$1.26{\cdot}10^{-5}$	27.01	$7.35{\cdot}10^{6}$	0.9997
KAR50	$3.65{\cdot}10^{-5}$	$2.72{\cdot}10^{-5}$	21.20	$3.04{\cdot}10^{6}$	0.9997
KAR60	$1.14{\cdot}10^{-4}$	$8.20{\cdot}10^{-5}$	22.91	$1.27{\cdot}10^{6}$	0.9995
KAR50S	$3.13{\cdot}10^{-5}$	$2.16{\cdot}10^{-5}$	24.20	$3.95{\cdot}10^{6}$	0.9997
CAP40	$1.01{\cdot}10^{-5}$	$9.32{\cdot}10^{-6}$	26.61	$8.95{\cdot}10^{6}$	0.9997
CAP50	$3.10{\cdot}10^{-5}$	$3.11{\cdot}10^{-5}$	24.79	$3.45{\cdot}10^{6}$	0.9995
CAP60	$9.42{\cdot}10^{-5}$	$8.18{\cdot}10^{-5}$	23.63	$1.14{\cdot}10^{6}$	0.9996
CAP50S	$2.26{\cdot}10^{-5}$	$1.88{\cdot}10^{-5}$	26.04	$4.86{\cdot}10^{6}$	0.9997
COM40	$1.53{\cdot}10^{-5}$	$1.43{\cdot}10^{-5}$	27.01	$6.47{\cdot}10^{6}$	0.9997
COM50	$4.42{\cdot}10^{-5}$	$3.05{\cdot}10^{-5}$	24.71	$3.24{\cdot}10^{6}$	0.9995
COM60	$1.20{\cdot}10^{-4}$	$8.63{\cdot}10^{-5}$	22.91	$1.20{\cdot}10^{6}$	0.9995
COM50S	$5.01{\cdot}10^{-5}$	$3.84{\cdot}10^{-5}$	23.45	$2.22{\cdot}10^{6}$	0.9996

related to the motions of different molecular structures. As W_CP is likely related to bound water and strongly correlated with γP, this could confirm that both β and γ relaxations are related to different water-bound molecular structures.

γ E_a is substantially not correlated with the protein and gluten content ($r < 0.12$). The moderate and negative correlation ($r = -0.47$) with the water amount could mean, similarly to the case of β relaxation, that water molecules can, at least in part, make the target group oscillation easier by interacting with it.

An additional relaxation process in COM and KAR samples (which have the highest gluten index), when salt was added, occurred at slightly lower temperatures and with consistently higher activation energy (80–90 kJ/mol). According to the literature (Butler & Cameron, 2000), this additional phenomenon is likely due to a regime of lower hydration with respect to the main relaxation, which prevails when the hydration increases, making the secondary relaxation undetectable. This is compatible with the presence of salt, which competes for water molecules with the starch.

Table 7
Correlation among the rheological, dielectric and composition parameters ([a] p-value ≤ 0.01; [b] 0.01 < p-value ≤ 0.05; [c] 0.05 < p-value ≤ 0.10 (WA:added water amount, PRO: protein content, GLU: gluten content, GI: gluten index, β E_a: β relaxation activation energy, γ E_a: γ relaxation activation energy, W_CP: water crystallization tan(δ) peak height, βP: β relaxation tan(δ) peak height, γP: γ relaxation tan(δ) peak height, J_0:instantaneous compliance, J_m: delayed compliance, τ: delay time and η_0: steady-state viscosity).

	WA	PRO	GLU	GI	β E_a	γ E_a	W_CP	βP	γP	J_0	J_m	τ	η_0
WA	1												
PRO	0	1											
GLU	0	**0.9954**[a]	1										
GI	0	**−0.9705**[a]	**−0.9891**[a]	1									
β Ea	−0.3098	−0.3613	−0.3773	0.3951	1								
γ Ea	−0.4734	−0.1181	−0.0849	0.0324	0.2589	1							
W_CP	−0.1824	**0.7722**[a]	**0.7764**[a]	**−0.7690**[a]	−0.2937	−0.2323	1						
βP	−0.2964	**0.7177**[a]	**0.7350**[a]	**−0.7483**[a]	0.0070	−0.0300	**0.7526**[a]	1					
γP	0.1764	0.3197	0.3597	−0.4147	−0.4383	−0.3697	**0.7133**[a]	0.3839	1				
J_0	**0.9131**[a]	−0.1320	−0.1453	0.1631	−0.0942	**−0.5684**[c]	−0.3273	−0.3099	0.0051	1			
J_m	**0.9166**[a]	−0.0308	−0.0414	0.0572	−0.1569	**−0.5870**[b]	−0.2461	−0.2171	0.05856	**0.9883**[a]	1		
τ	**−0.7460**[a]	0.3278	0.3210	−0.3047	0.4488	0.3301	0.4860	**0.5408**[c]	0.0303	**−0.6478**[b]	**−0.6203**[b]	1	
η_0	**−0.9287**[a]	0.1501	0.1649	−0.1848	0.3619	0.4687	0.3015	0.4588	−0.0727	**−0.8249**[a]	**−0.8261**[a]	**0.8233**[a]	1

4.4. Relationship between dielectric and rheological response

Looking at correlation coefficients in Table 7, the first considerations should be done about the relationships between the Burgers model parameters. J_0 and J_m are very strongly and significantly correlated ($r = 0.99$), meaning that they are representative of, and influenced by, the same conditions in the dough. η_0 is significantly correlated with all the other Burgers parameters, even if a little more slightly ($r \in [-0.83, -0.82]$, while τ shows weaker, but still significant correlations with J_0 and J_m ($r \in [-0.65, -0.62]$).

All the Burgers parameters are significantly correlated with the water content, with r = 0.91–0.92 for J_0 and J_m, – 0.92 for η_0, and – 0.75 for τ. However, no one of them is significantly correlated to protein and gluten amount, nor to the gluten index, and the correlation coefficients are in general low, especially for J_0, J_m and η_0. This could lead to the erroneous conclusion that the semolina composition does not affect the creep response of the dough and that the water amount is the only parameter that influences the rheological behaviour. Actually, the composition alone cannot completely explain the rheological behaviour, but not even the water amount alone, because it is well known that the result depends on the complex interactions among all the dough components.

In effect, looking at the correlations between the Burgers parameters and the dielectric ones, the latter reveal to be much more informative about the effects of the molecular dynamics in the dough on its rheological response. J_0 and J_m present a significant, negative, and stronger correlation with $\gamma\ E_a$ ($r \in [-0.58, -0.56]$) when compared to the semolina composition parameters. Correlations with W_CP and βP are weaker if compared to the previous one (respectively $r \in [-0.33, -0.25]$ and $r \in [-0.31, -0.22]$). However, they show to be higher than those with the semolina composition parameters. J_0 and J_m are not correlated with $\beta\ E_a$ ($r \in [-0.16, -0.09]$), nor with γP ($r \in [-0.06, -0.01]$). τ is significantly, even if not very strongly, correlated with βP (r = 0.54). τ also presents a moderate correlation value (r = 0.49) with W_CP, and weaker correlations with $\beta\ E_a$ and $\gamma\ E_a$ (r = 0.45 and r = 0.33, respectively). No correlation was found between τ and γP (r = 0.03). η_0 is the only Burgers parameter which does not present significant correlations with dielectric parameters. However, medium correlation coefficients were found with respect to $\beta\ E_a$ and $\gamma\ E_a$ (r = 0.36 and r = 0.47, respectively), to W_CP and βP (r = 0.30 and r = 0.46, respectively). No correlation was found between η_0 and γP (r = – 0.07).

In summary, $\gamma\ E_a$ could give the most significant information on J_0 and J_m, βP is the most significant dielectric parameter with respect to τ, while no dielectric parameter is suitable to give significant information on η_0. γP revealed to be substantially uncorrelated with respect to all Burgers parameters, thus not informative on the dough rheological behaviour.

Looking at the supposed explanations of the dielectric relaxations, the starch hydration, at the glucose ring level, could be responsible, to a certain extent, of the dough compliance, as far as the water molecules are able to make the molecular movements easier, regardless the actual amount of bound water. On the other hand, the amount of hydroxyl groups in the glucosidic units of starch can act as a retardant of the dough deformation, as an increasing amount of them makes the rheological delay time increase. A similar effect is likely produced on the dough viscosity, even if the correlation with the dielectric parameters is not statistically significant.

5. Conclusions

This work aimed to investigate the dielectric properties of semolina doughs and to find connections with their rheological properties. The goal was to develop a characterization technique able to give information on the process conditions of industrial bakery products and pasta concerning their quality properties in manufacturing and freezing processes.

It was observed that semolina dough displays three molecular relaxation phenomena: the water crystallization process, β and γ relaxations.

Water crystallization occurred in the temperature range between 0 and -10 °C. This process showed to be mostly related to the bound water in the system and to the interactions that it establishes with other molecules in the dough.

The β relaxation occurred in the temperature range between −40 °C and −70 °C and showed activation energy of about 50–75 kJ/mol. This process is probably associated with relaxations in glucosidic units, due to the rotational motion of the hydroxyl groups present on carbon atoms (C_2, C_3, or C_6).

The γ relaxation occurred in the temperature range between −115 °C and −100 °C and showed activation energy of about 30–40 kJ/mol. This process is likely due to localized chain motions in starch molecules, probably small amplitude oscillations of the glucose rings about the (1–4)-α and (1–6)-α linkages enabled by hydrogen bound water.

When salt is added to the dough, it is possible to observe an additional relaxation process at slightly lower temperatures and with consistently higher activation energy (80–90 kJ/mol) than the γ one. This additional phenomenon is likely due to a regime of lower hydration compatible with the presence of salt. For the same reason, NaCl is also able to reduce the transition temperatures of the unfrozen solute, producing a temperature shifting in the β relaxation.

Concerning the rheological aspects, the Burgers parameters presented a strong correlation with the water amount, while they were very slightly correlated with the protein and gluten amount. On the other hand, much higher correlations were found between Burgers and most of the dielectric parameters, obtained at sub-zero temperatures, revealing that the latter can be very informative in explaining, to a certain extent, the rheological properties of the dough. Finally, no relationship between the γ relaxation tan(δ) peak height and the dough compliance was found in this study.

CRediT authorship contribution statement

Fabio Fanari: Methodology, Software, Investigation, Data curation, Writing – original draft, Visualization. **Ciprian Iacob:** Methodology, Validation, Data curation. **Gianluca Carboni:** Resources, Investigation. **Francesco Desogus:** Conceptualization, Methodology, Writing – review & editing, Funding acquisition. **Massimiliano Grosso:** Conceptualization, Software, Formal analysis, Project administration. **Manfred Wilhelm:** Resources, Supervision.

Declaration of competing interest

The authors declare that they have no known competing financial interests or personal relationships that could have appeared to influence the work reported in this paper.

Acknowledgments

This research was partly funded by Italian Government (Ministero dello Sviluppo Economico), Fondo per la Crescita Sostenibile – Sportello "Agrifood" PON I&C 2014–2020, Prog. n. F/200133/01–03/X45. The authors would like to thank Dr. Christopher Klein (Karlsruher Institut für Technologie) for his precious support in the rheological measurements.

Appendix A

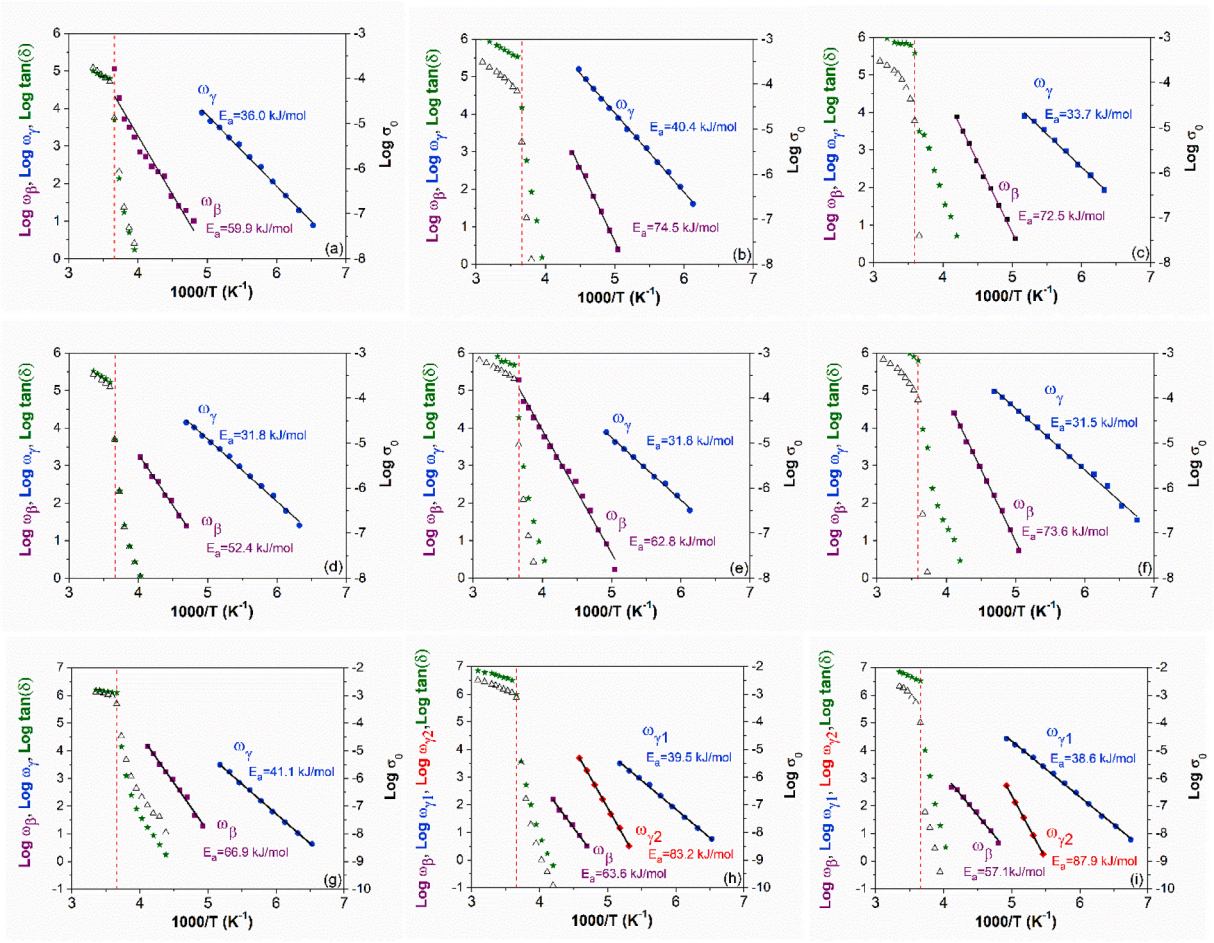

Fig. A.1. mobility map and Arrhenius model regression with E_a values for samples with 40 wt% amount of water CAP40 (a), KAR40 (b), COM40 (c), 60 wt% amount of water CAP60 (d), KAR60 (e), COM60 (f), 50 wt% amount of water and 1.5 wt% amount of salt CAP50S (g), KAR50S (h), COM50S (i) samples. Triangles represent tan(δ) while green stars σ_0 values. The red dashed line highlights the crystallization temperature, in correspondence of which a drop in tan(δ) is observable

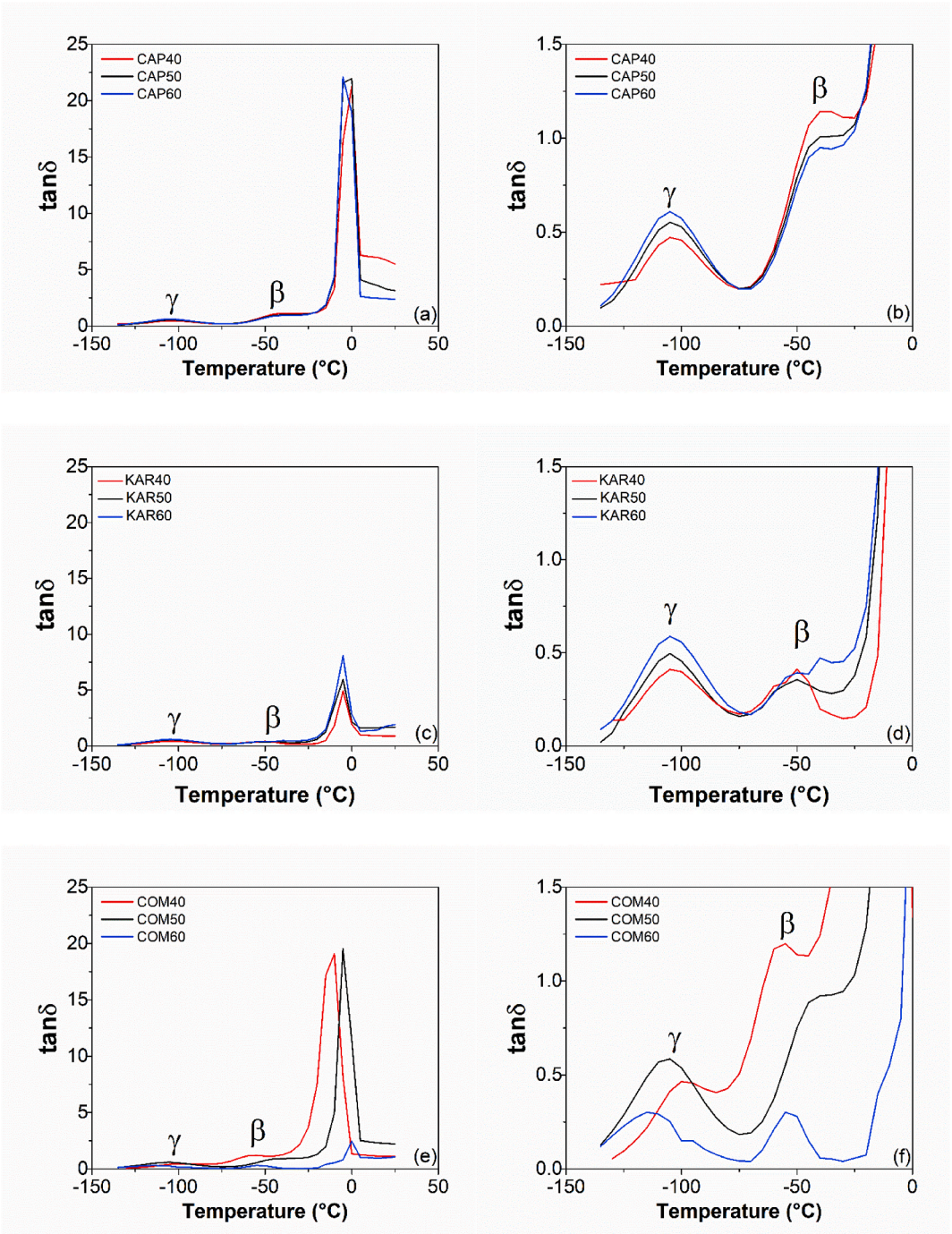

Fig. A.2. tan(δ) as a function of temperature (a) and enlargement of the β and γ relaxations zone (b) for CAP40, CAP50, and CAP60 samples; tan(δ) as a function of temperature (c) and enlargement of the β and γ relaxations zone (d) for KAR40, KAR50, and KAR60 samples; tan(δ) as a function of temperature (e) and enlargement of the β and γ relaxations zone (f) for COM40, COM50, and COM60 samples. All data reported were measured at the frequency of 100 Hz

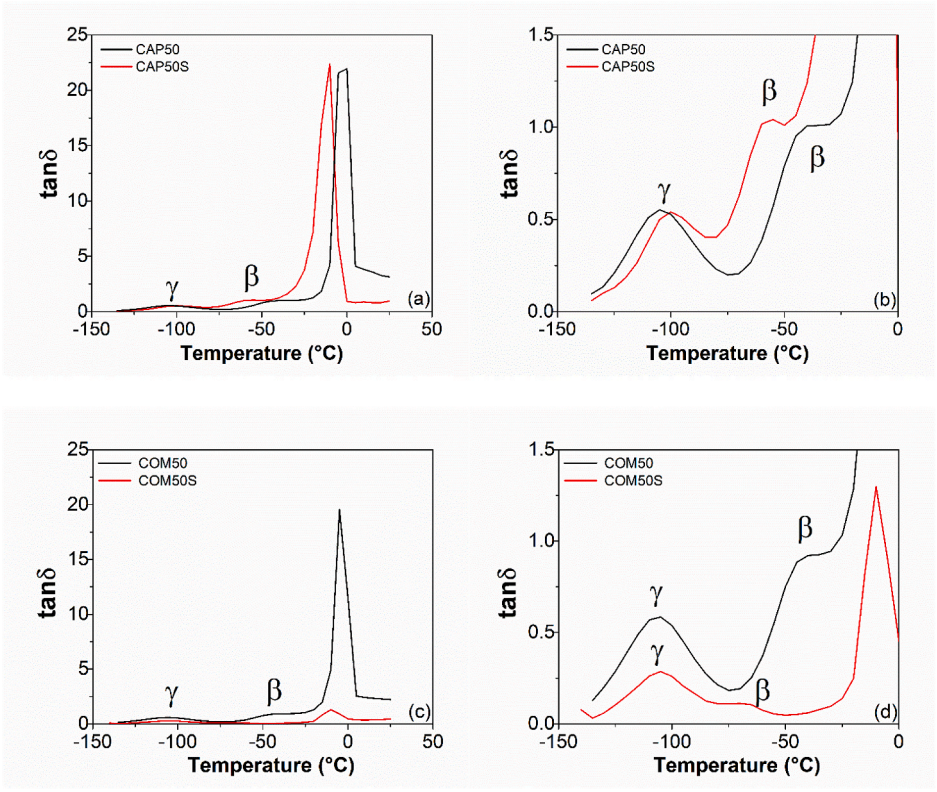

Fig. A.3. tan(δ) as a function of temperature (a) and enlargement of the β and γ relaxations zone (b) for CAP50 and CAP50S samples; tan(δ) as a function of temperature (c) and enlargement of the β and γ relaxations zone (d) for COM50 and COM50S samples. All data reported were measured at the frequency of 100 Hz

References

Akbarian, M., Koocheki, A., Mohebbi, M., & Milani, E. (2016). Rheological properties and bread quality of frozen sweet dough with added xanthan and different freezing rate. *Journal of Food Science & Technology, 53*(10), 3761–3769. https://doi.org/10.1007/s13197-016-2361-2

Balasubramanian, S., Devi, A., Singh, K. K., D Bosco, S. J., & Mohite, A. M. (2016). Application of glass transition in food processing. *Critical Reviews in Food Science and Nutrition, 56*(6), 919–936. https://doi.org/10.1080/10408398.2012.734343

Barak, S., Mudgil, D., & Khatkar, B. S. (2013). Relationship of gliadin and glutenin proteins with dough rheology, flour pasting and bread making performance of wheat varieties. *Lebensmittel-Wissenschaft und -Technologie- Food Science and Technology, 51*(1), 211–217. https://doi.org/10.1016/j.lwt.2012.09.011

Barak, S., Mudgil, D., & Khatkar, B. S. (2014). Influence of gliadin and glutenin fractions on rheological, pasting, and textural properties of dough. *International Journal of Food Properties, 17*(7), 1428–1438. https://doi.org/10.1080/10942912.2012.717154

Beck, M., Jekle, M., & Becker, T. (2012). Impact of sodium chloride on wheat flour dough for yeast-leavened products. I. Rheological attributes. *Journal of the Science of Food and Agriculture, 92*(3), 585–592. https://doi.org/10.1002/jsfa.4612

Bibi, F., Villain, M., Guillaume, C., Sorli, B., & Gontard, N. (2016). A review: Origins of the dielectric properties of proteins and potential development as bio-sensors. *Sensors, 16*(8), 1232. https://doi.org/10.3390/s16081232

Böhmer, R., Chamberlin, R. V., Diezemann, G., Geil, B., Heuer, A., Hinze, G., et al. (1998). Nature of the non-exponential primary relaxation in structural glass-formers probed by dynamically selective experiments. *Journal of Non-crystalline Solids, 235–237*, 1–9. https://doi.org/10.1016/S0022-3093(98)00581-X

Bonilla, J. C., Erturk, M. Y., & Kokini, J. L. (2020). Understanding the role of gluten subunits (LMW, HMW glutenins and gliadin) in the networking behavior of a weak soft wheat dough and a strong semolina wheat flour dough and the relationship with linear and non-linear rheology. *Food Hydrocolloids, 108*, 106002. https://doi.org/10.1016/j.foodhyd.2020.106002

Bonilla, J. C., Erturk, M. Y., Schaber, J. A., & Kokini, J. L. (2020). Distribution and function of LMW glutenins, HMW glutenins, and gliadins in wheat doughs analyzed with 'in situ' detection and quantitative imaging techniques. *Journal of Cereal Science, 93*, 102931. https://doi.org/10.1016/j.jcs.2020.102931

Bonilla, J. C., Schaber, J. A., Bhunia, A. K., & Kokini, J. L. (2019). Mixing dynamics and molecular interactions of HMW glutenins, LMW glutenins, and gliadins analyzed by fluorescent co-localization and protein network quantification. *Journal of Cereal Science, 89*, 102792. https://doi.org/10.1016/j.jcs.2019.102792

Brandner, S., Becker, T., & Jekle, M. (2019). Classification of starch-gluten networks into a viscoelastic liquid or solid, based on rheological aspects — a review. In *International journal of biological macromolecules* (Vol. 136, pp. 1018–1025). Elsevier B.V. https://doi.org/10.1016/j.ijbiomac.2019.06.160.

Butler, M. F., & Cameron, R. E. (2000). A study of the molecular relaxations in solid starch using dielectric spectroscopy. *Polymer, 41*(6), 2249–2263. https://doi.org/10.1016/S0032-3861(99)00366-3

Chan, R. K., Pathmanathan, K., & Johari, G. P. (1986). Dielectric relaxations in the liquid and glassy states of glucose and its water mixtures. *Journal of Physical Chemistry, 90*(23), 6358–6362. https://doi.org/10.1021/j100281a059

Ding, X., Zhang, H., Wang, L., Qian, H., Qi, X., & Xiao, J. (2015). Effect of barley antifreeze protein on thermal properties and water state of dough during freezing and freeze-thaw cycles. *Food Hydrocolloids, 47*, 32–40. https://doi.org/10.1016/j.foodhyd.2014.12.025

Döring, C., Nuber, C., Stukenborg, F., Jekle, M., & Becker, T. (2015). Impact of arabinoxylan addition on protein microstructure formation in wheat and rye dough. *Journal of Food Engineering, 154*, 10–16. https://doi.org/10.1016/j.jfoodeng.2014.12.019

Edwards, N. M., Dexter, J. E., & Scanlon, M. G. (2002). Starch participation in durum dough linear viscoelastic properties. *Cereal Chemistry, 79*(6), 850–856. https://doi.org/10.1094/CCHEM.2002.79.6.850

Fanari, F., Carboni, G., Grosso, M., & Desogus, F. (2020). Thermal properties of semolina doughs with different relative amount of ingredients. *Sustainability, 12*(6), 2235. https://doi.org/10.3390/su12062235

Fanari, F., Desogus, F., Scano, E. A., Carboni, G., & Grosso, M. (2020). The effect of the relative amount of ingredients on the rheological properties of semolina doughs. *Sustainability, 12*(7), 2705. https://doi.org/10.3390/su12072705

Fanari, F., Frau, I., Desogus, F., Scano, E. A., Carboni, G., & Grosso, M. (2019). Influence of wheat varieties, mixing time and water content on the rheological properties of semolina doughs. *Chemical Engineering Transactions, 75*, 529–534. https://doi.org/10.3303/CET1975089

Fanari, F., Muntoni, G., Dachena, C., Carta, R., & Desogus, F. (2020). Microwave heating improvement: Permittivity characterization of water–ethanol and water–NaCl binary mixtures. *Energies, 13*(18). https://doi.org/10.3390/en13184861

Ficco, D. B. M., Saia, S., Beleggia, R., Fragasso, M., Giovanniello, V., & De Vita, P. (2017). Milling overrides cultivar, leavening agent and baking mode on chemical and rheological traits and sensory perception of durum wheat breads. *Scientific Reports, 7*(1). https://doi.org/10.1038/s41598-017-14113-5

Goedeken, D. L., Tong, C. H., & Virtanen, A. J. (1997). Dielectric properties of a pregelatinized bread system at 2450 MHz as a function of temperature, moisture, salt and specific volume. *Journal of Food Science, 62*(1), 145–149. https://doi.org/10.1111/j.1365-2621.1997.tb04387.x

Havriliak, S., & Negami, S. (1967). A complex plane representation of dielectric and mechanical relaxation processes in some polymers. *Polymer, 8*(C), 161–210. https://doi.org/10.1016/0032-3861(67)90021-3

Heuer, A., Wilhelm, M., Zimmermann, H., & Spiess, H. W. (1995). Rate memory of structural relaxation in glasses and its detection by multidimensional NMR. *Physical Review Letters, 75*(15), 2851–2854. https://doi.org/10.1103/PhysRevLett.75.2851

Hyun, K., Höfl, S., Kahle, S., & Wilhelm, M. (2009). Polymer motion as detected via dielectric spectra of 1,4-cis-polyisoprene under large amplitude oscillatory shear (Laos). *Journal of Non-newtonian Fluid Mechanics, 160*(2–3), 93–103. https://doi.org/10.1016/j.jnnfm.2009.03.002

Iacob, C., Yoo, T., & Runt, J. (2018). Molecular dynamics of polyfarnesene. *Macromolecules, 51*(13), 4917–4922. https://doi.org/10.1021/acs.macromol.8b00851

ICC. (1995). *Gluten index method for assessing gluten strength in durum wheat (Triticum durum)* (Vol. 158).

ISO 16634-2:2016. (2016). *Food products — determination of the total nitrogen content by combustion according to the Dumas principle and calculation of the crude protein content — Part 2: Cereals, pulses and milled cereal products*.

Kang, W., Lu, J., Cheng, Y., & Jin, Y. (2015). Determination of the concentration of alum additive in deep-fried dough sticks using dielectric spectroscopy. *Journal of Food and Drug Analysis, 23*(3), 472–479. https://doi.org/10.1016/j.jfda.2014.10.003

Kim, Y. R., & Cornillon, P. (2001). Effects of temperature and mixing time on molecular mobility in wheat dough. *Lebensmittel-Wissenschaft und -Technologie- Food Science and Technology*. https://doi.org/10.1006/fstl.2000.0717

Laaksonen, T. J., Kuuva, T., Jouppila, K., & Roos, Y. H. (2002). Effects of arabinoxylans on thermal behavior of frozen wheat doughs as measured by DSC, DMA, and DEA. *Journal of Food Science, 67*(1), 223–230. https://doi.org/10.1111/j.1365-2621.2002.tb11388.x

Laaksonen, T. J., & Roos, Y. H. (2000). Thermal, dynamic-mechanical, and dielectric analysis of phase and state transitions of frozen wheat doughs. *Journal of Cereal Science, 32*(3), 281–292. https://doi.org/10.1006/jcrs.2000.0338

Laaksonen, T. J., & Roos, Y. H. (2001a). Dielectric relaxations of frozen wheat doughs containing sucrose, NaCl, ascorbic acid and their mixtures. *Journal of Cereal Science*. https://doi.org/10.1006/jcrs.2001.0370

Laaksonen, T. J., & Roos, Y. H. (2001b). Thermal and dynamic-mechanical properties of frozen wheat doughs with added sucrose, NaCl, ascorbic acid, and their mixtures. *International Journal of Food Properties, 4*(2), 201–213. https://doi.org/10.1081/JFP-100105187

Laaksonen, T. J., & Roos, Y. H. (2003). Water sorption and dielectric relaxations of wheat dough (containing sucrose, NaCl, and their mixtures). *Journal of Cereal Science*. https://doi.org/10.1006/jcrs.2002.0506

Levine, H., & Slade, L. (1990). Influences of the glassy and rubbery states on the thermal, mechanical, and structural properties of doughs and baked products. In *Dough rheology and baked product texture*. https://doi.org/10.1007/978-1-4613-0861-4_5, 157–330.

Li, L., Zhang, M., & Yang, P. (2019). Suitability of LF-NMR to analysis water state and predict dielectric properties of Chinese yam during microwave vacuum drying. *Lebensmittel-Wissenschaft & Technologie, 105*, 257–264. https://doi.org/10.1016/j.lwt.2019.02.017

Mainardi, F., & Spada, G. (2011). Creep, relaxation and viscosity properties for basic fractional models in rheology. *The European Physical Journal - Special Topics, 193*(1), 133–160. https://doi.org/10.1140/epjst/e2011-01387-1

Matuda, T. G., Pessôa Filho, P. A., & Tadini, C. C. (2011). Experimental data and modeling of the thermodynamic properties of bread dough at refrigeration and freezing temperatures. *Journal of Cereal Science, 53*(1), 126–132. https://doi.org/10.1016/j.jcs.2010.11.002

Mefleh, M., Conte, P., Fadda, C., Giunta, F., Piga, A., Hassoun, G., et al. (2019). From ancient to old and modern durum wheat varieties: Interaction among cultivar traits, management, and technological quality. *Journal of the Science of Food and Agriculture, 99*(5), 2059–2067. https://doi.org/10.1002/jsfa.9388

Meins, T., Dingenouts, N., Kübel, J., & Wilhelm, M. (2012). In situ rheodielectric, ex situ 2D-SAXS, and Fourier transform rheology investigations of the shear-induced alignment of poly(styrene-b-1,4-isoprene) diblock copolymer melts. *Macromolecules, 45*(17), 7206–7219. https://doi.org/10.1021/ma300124b

Meziani, S., Jasniewski, J., Gaiani, C., Ioannou, I., Muller, J. M., Ghoul, M., et al. (2011). Effects of freezing treatments on viscoelastic and structural behavior of frozen sweet dough. *Journal of Food Engineering, 107*(3–4), 358–365. https://doi.org/10.1016/j.jfoodeng.2011.07.003

Migliori, M., & Gabriele, D. (2010). Effect of pentosan addition on dough rheological properties. *Food Research International, 43*(9), 2315–2320. https://doi.org/10.1016/j.foodres.2010.08.008

Miller, R. A., & Hoseney, R. C. (2008). Role of salt in baking. *Cereal Foods World, 53*(1), 4–6. https://doi.org/10.1094/CFW-53-1-0004

Mironeasa, S., & Codină, G. G. (2019). Dough rheological behavior and microstructure characterization of composite dough with wheat and tomato seed flours. *Foods, 8*(12). https://doi.org/10.3390/foods8120626

Moreira, R., Chenlo, F., Torres, M. D., & Rama, B. (2014). Fine particle size chestnut flour doughs rheology: Influence of additives. *Journal of Food Engineering, 120*(1), 94–99. https://doi.org/10.1016/j.jfoodeng.2013.07.025

Nielsen, G. G. B., Kjær, A., Klösgen, B., Hansen, P. L., Simonsen, A. C., & Jørgensen, B. (2016). Dielectric spectroscopy for evaluating dry matter content of potato tubers. *Journal of Food Engineering, 189*, 9–16. https://doi.org/10.1016/j.jfoodeng.2016.05.011

Oikonomou, N. A., Bakalis, S., Rahman, M. S., & Krokida, M. K. (2015). Gluten index for wheat products: Main variables in affecting the value and nonlinear regression model. *International Journal of Food Properties, 18*(1), 1–11. https://doi.org/10.1080/10942912.2013.772198

Pandino, G., Mattiolo, E., Lombardo, S., Lombardo, G. M., & Mauromicale, G. (2020). Organic cropping system affects grain chemical composition, rheological and agronomic performance of durum wheat. *Agriculture, 10*(2). https://doi.org/10.3390/agriculture10020046

Perera, D. Y. (2002). Effect of thermal and hygroscopic history on physical ageing of organic coatings. *Progress in Organic Coatings, 44*(1), 55–62. https://doi.org/10.1016/S0300-9440(01)00241-7

Phan-Thien, N., & Safari-Ardi, M. (1998). Linear viscoelastic properties of flour-water doughs at different water concentrations. *Journal of Non-newtonian Fluid Mechanics, 74*(1–3), 137–150. https://doi.org/10.1016/S0377-0257(97)00071-2

Popov, I., Ishai, P. B., Khamzin, A., & Feldman, Y. (2016). The mechanism of the dielectric relaxation in water. *Physical Chemistry Chemical Physics, 18*, 13941. https://doi.org/10.1039/c6cp02195f

Ribotta, P. D., & Le Bail, A. (2007). Effect of additives on the thermo-mechanical behaviour of dough systems at sub-freezing temperatures. *European Food Research and Technology, 224*(4), 519–524. https://doi.org/10.1007/s00217-006-0331-z

Roos, Y. (1993). Melting and glass transitions of low molecular weight carbohydrates. *Carbohydrate Research, 238*(C), 39–48. https://doi.org/10.1016/0008-6215(93)87004-C

Roudaut, G., Maglione, M., & Le Meste, M. (1999). Relaxations below glass transition temperature in bread and its components. *Cereal Chemistry, 76*(1), 78–81. https://doi.org/10.1094/CCHEM.1999.76.1.78

Roudaut, G., Maglione, M., Van Dusschoten, D., & Le Meste, M. (1999). Molecular mobility in glassy bread: A multispectroscopy approach. *Cereal Chemistry, 76*(1), 70–77. https://doi.org/10.1094/CCHEM.1999.76.1.70

Roudaut, G., Simatos, D., Champion, D., Contreras-Lopez, E., & Le Meste, M. (2004). Molecular mobility around the glass transition temperature: A mini review. *Innovative Food Science & Emerging Technologies, 5*(2), 127–134. https://doi.org/10.1016/j.ifset.2003.12.003

Scandola, M., Ceccorulli, G., & Pizzoli, M. (1991). Molecular motions of polysaccharides in the solid state: Dextran, pullulan and amylose. *International Journal of Biological Macromolecules, 13*(4), 254–260. https://doi.org/10.1016/0141-8130(91)90082-6

Schönhals, A., & Kremer, F. (2003). Theory of dielectric relaxation. In *Broadband dielectric spectroscopy* (pp. 1–33). Springer Berlin Heidelberg. https://doi.org/10.1007/978-3-642-56120-7_1.

Sicignano, A., Di Monaco, R., Masi, P., & Cavella, S. (2015). From raw material to dish: Pasta quality step by step. *Journal of the Science of Food and Agriculture, 95*(13), 2579–2587. https://doi.org/10.1002/jsfa.7176

Slade, L., & Levine, H. (1995). Water and the glass transition - dependence of the glass transition on composition and chemical structure: Special implications for flour functionality in cookie baking. *Journal of Food Engineering, 24*(4), 431–509. https://doi.org/10.1016/0260-8774(95)90766-5

Steeman, P. A. M., & van Turnhout, J. (1994). Fine structure in the parameters of dielectric and viscoelastic relaxations. *Macromolecules, 27*(19), 5421–5427. https://doi.org/10.1021/ma00097a023

Sun, X., Koksel, F., Nickerson, M. T., & Scanlon, M. G. (2020). Modeling the viscoelastic behavior of wheat flour dough prepared from a wide range of formulations. *Food Hydrocolloids, 98*, 105129. https://doi.org/10.1016/j.foodhyd.2019.05.030

Torbica, A., Mocko Blažek, K., Belović, M., & Janić Hajnal, E. (2019). Quality prediction of bread made from composite flours using different parameters of empirical rheology. *Journal of Cereal Science, 89*. https://doi.org/10.1016/j.jcs.2019.102812

Tracht, U., Wilhelm, M., Heuer, A., Feng, H., Schmidt-Rohr, K., & Spiess, H. W. (1998). Length scale of dynamic heterogeneities at the glass transition determined by multidimensional nuclear magnetic resonance. *Physical Review Letters, 81*(13), 2727–2730. https://doi.org/10.1103/PhysRevLett.81.2727

Volkov, A. S., Koposov, G. D., Perfil'ev, R. O., & Tyagunin, A. V. (2018). Analysis of experimental results by the havriliak–negami model in dielectric spectroscopy. *Optics and Spectroscopy, 124*(2), 202–205. https://doi.org/10.1134/S0030400X18020200

Wang, Y., & Zhou, W. (2017). Non-equilibrium states and glass transitions in bakery products. *Non-Equilibrium States and Glass Transitions in Foods: Processing Effects and Product-Specific Implications*, 63–87. https://doi.org/10.1016/B978-0-08-100309-1.00005-5

Wübbenhorst, M., & Van Turnhout, J. (2002). Analysis of complex dielectric spectra. I: One-dimensional derivative techniques and three-dimensional modelling. *Journal of Non-crystalline Solids, 305*(1–3), 40–49. https://doi.org/10.1016/S0022-3093(02)01086-4

Yang, Y., Zheng, S., Li, Z., Pan, Z., Huang, Z., Zhao, J., et al. (2021). Influence of three types of freezing methods on physicochemical properties and digestibility of starch in frozen unfermented dough. *Food Hydrocolloids, 115*, 106619. https://doi.org/10.1016/J.FOODHYD.2021.106619